SAND2008-2499C

Nano-Scale Tribological Behavior of Polycrystalline Silicon Structural Films in Ambient Air

Daan Hein Alsem[1], Ruben van der Hulst[2], Eric A. Stach[3], Michael T. Dugger[4], Jeff Th. M. de Hosson[2], and Robert O. Ritchie[1,5]

[1]Materials Sciences Division, Lawrence Berkeley National Laboratory, Berkeley, CA, 94720
[2]Department of Applied Physics, University of Groningen, Groningen, 9747 AG, Netherlands
[3]School of Materials Engineering and Birck Nanotechnology Center, Purdue University, West Lafayette, IN, 47907
[4]Materials Science and Engineering Center, Sandia National Laboratories, Albuquerque, NM, 87185
[5]Department of Materials Science and Engineering, University of California at Berkeley, Berkeley, CA, 94720

ABSTRACT

Dynamic friction, wear volumes and wear morphology have been studied for sliding wear in polysilicon in ambient air at μN normal loads using on-chip micron-scale test specimens. With increasing number of wear cycles, the friction coefficients show two distinct types of behavior: (i) an increase by a factor of two and a half to a steady-state regime after peaking at three times the initial value of about 0.10 ± 0.04, with no failure after millions of cycles; (ii) an increase by a factor larger than three followed by failure after $\sim 10^5$ cycles. Additionally, the average nano-scale wear coefficient sharply increased in the first $\sim 10^5$ cycles up to about 10^{-4} and then decayed by an order of magnitude over the course of several million cycles. For both modes of behavior, abrasive wear is the governing mechanism, the difference being attributed to variations in the local surface morphology (and wear debris) between the sliding surfaces. The oxidation of worn polysilicon surfaces only affects the friction coefficient after periods of inactivity (>30 min).

INTRODUCTION

Microelectromechanical systems (MEMS) can be fabricated at low cost using batch processing; they are found in a wide variety of consumer products and defence/space applications like sensors, projection displays, inkjet printers and optical switches [1,2]. Due to their large surface-to-volume ratio, it not always possible to simply extrapolate known macro-scale failure modes to MEMS on the micro- and nano-meter scale. Although a growing amount of research has provided insight into how to overcome problems in their fabrication and design [2], MEMS can fail prematurely by such failure modes as adhesion, wear and fatigue [3]. Adhesion and wear are more common in devices with contacting surfaces (see recent review [4]), but fatigue is of particular interest for silicon MEMS because large-scale specimens of silicon are not susceptible to this failure mode [5]. In this paper, we measure the dynamic coefficient of friction and nano-scale wear volumes as function of wear cycles in order to gain more insight in the evolution of friction and wear of polycrystalline silicon (polysilicon) sidewalls during wear. Furthermore, we use the static friction coefficient to investigate re-oxidation of worn polysilicon sidewall surfaces. Results are discussed in terms of the physical mechanisms active during the wear process.

EXPERIMENTAL METHODS

On-chip n^+-type polysilicon sidewall friction and wear test specimens were fabricated using the Sandia SUMMiT V™ fabrication process [6]. A 1H,1H,2H,2H-perflurordecyltrichlorosilane (FDTS) monolayer coating was deposited during release [7] to reduce unintentional adhesion of freestanding elements. The device (Fig. 1) consists of two suspended shuttles, the normal and tangential shuttle (Fig. 1a). Each shuttle is driven laterally by an electrostatic comb drive (Figure 1a). By applying a DC voltage to the normal comb drive, the beam is pushed against the post (Fig. 1b). Sinusoidal AC signals are applied to the tangential comb drive causing wearing of the beam against the post (Fig. 1b). The average normal force between the post and the beam is determined by a calibration as described in [8,9]. Static coefficients of friction are determined by applying a normal force to cause the beam to make contact with the post; the tangential force is ramped up by a DC voltage signal (~ 1 V/s) until the beam slips along the post [8,9].

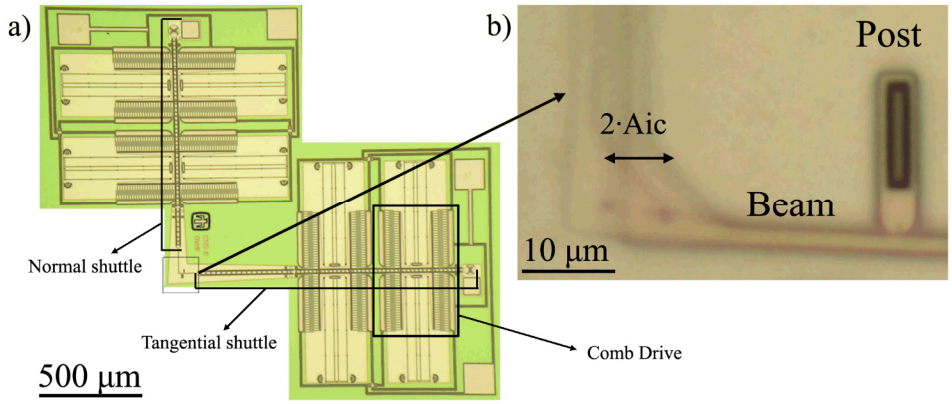

Figure 1: Optical micrographs showing an overview of a sidewall friction test device (a) and beam and post contact while the device is in motion (b).

The average dynamic coefficient of friction is defined as the ratio of the dynamic friction force to the applied normal force ($\mu_d = F_{friction} / F_N$). While the latter is known from the calibration, the former is obtained by comparing the amplitude of the beam out of contact with the post (A_{oc}) and the amplitude in contact with the post (A_{ic}) [10]. The average dynamic friction force is then given by $F_{friction} = (A_{oc} - A_{ic}) \cdot (k_b' + k_c)$, where k_b' is the effective spring constant of the normal beam and k_c the effective spring constant of the folded beam suspension internal to the tangential comb drive [8,9].

All devices were operated in ambient air (20-35% relative humidity, 23-27 °C) under a normal contact force of 2-3 µN at 100 Hz with sliding peak-to-peak amplitude of 5-7 µm. At these small scales, adhesive forces, *e.g.*, Van der Waals, can be of the same order of magnitude as external forces. To account for them, an upper bound for the adhesion force with this contact geometry (apparent contact area of 0.1-0.5 μm^2) was determined to be 0.16 µN.

Scanning electron microscopy (SEM) imaging (JEOL 6340F at 20 kV) was employed to determine the wear morphology. Atomic-force microscopy (AFM; Asylum Research MFP-3D) was used to determine nano-scale wear volumes. Details are provided elsewhere [9].

RESULTS

Friction

The dynamic coefficient of friction displayed two different types of behavior. Some devices are able to cycle for millions of cycles (Mode I), while other devices stop functioning significantly earlier (~89,000 cycles, designated Mode II). A total of 7 devices tested under similar operating conditions led to the observation of these two modes of behavior. Averaging over several devices, the initial dynamic coefficient of friction started at 0.10 ± 0.04 and for Mode I devices reached a peak value of 0.31 ± 0.11 at 103,000 ± 24,000 cycles. Subsequently, the coefficient of friction decreased slightly to reach a steady-state value of 0.25 ± 0.10. This Mode I type of behavior is shown for one particular device in Fig. 2.

For devices exhibiting Mode II behaviour, the dynamic coefficient of friction also started at 0.10 ± 0.04, but rose continually to a peak value of 0.35 ± 0.07 and failed after 89,000 ± 4,000 cycles. This Mode II type of behavior is shown for one particular device in Fig. 3.

To look at the effect of (re-)oxidation during the wear process, devices were run to over 500,000 cycles and then stopped, after which the static coefficient of friction was periodically measured. Fig. 4 shows how that the static coefficient of friction stays approximately constant up to about 30 minutes after the device was stopped, after which it decreases in the next 1,000 minutes before reaching a steady-state at a value, approximately two times lower than the maximum coefficient of friction and only slightly higher than the initial value (0.12 ± 0.02 [9]).

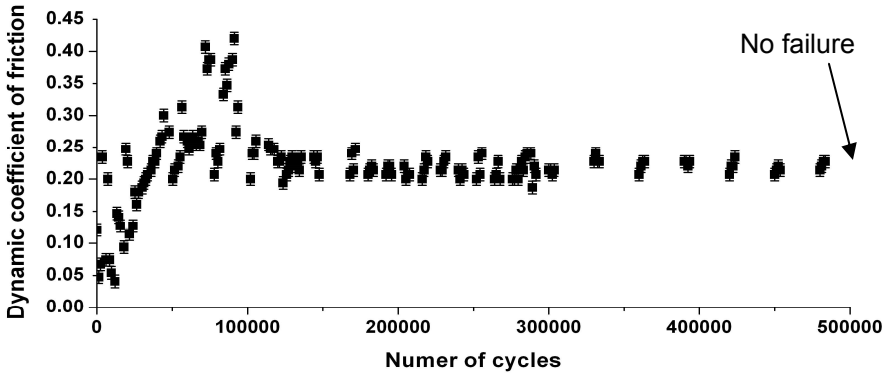

Figure 2: Typical example of results for the dynamic coefficient of friction as a function of number of cycles, for a device run at a normal force of 2.1 μN, displaying Mode I behavior (stopped after 500,000 cycles without failure).

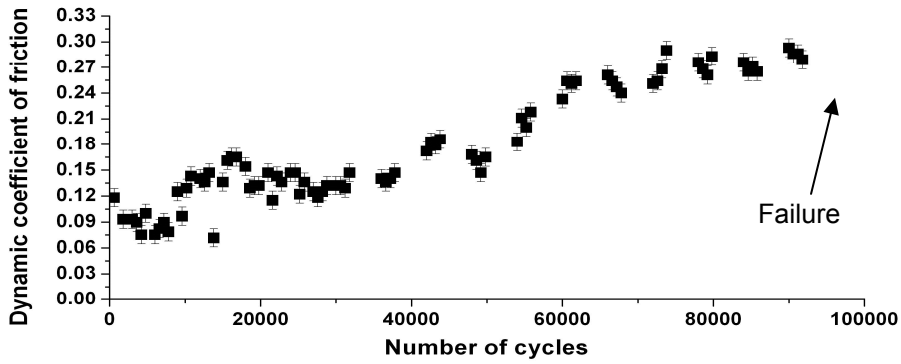

Figure 3: Corresponding results of the dynamic coefficient of friction *vs.* number of cycles for a sidewall friction device displaying Mode II behavior (run at a normal force of 2.9 μN).

Wear

From the SEM micrographs in Fig. 5, one can see that there is no large differences in the wear morphology when comparing Mode I and II devices.

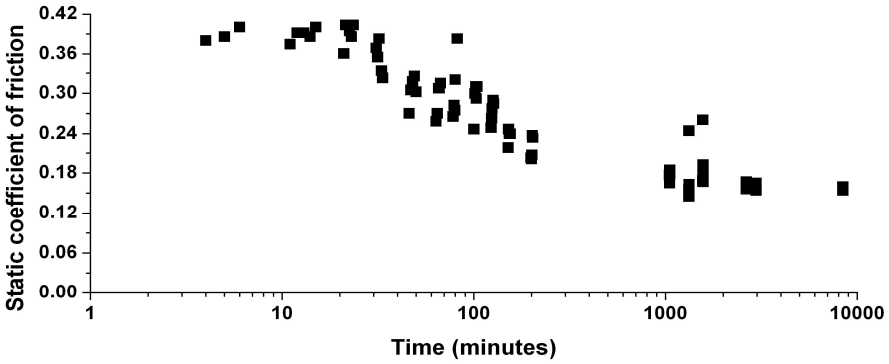

Figure 4: Static coefficient of friction versus time after a device has been run for 700,000 cycles (F_N = 2.1 μN).

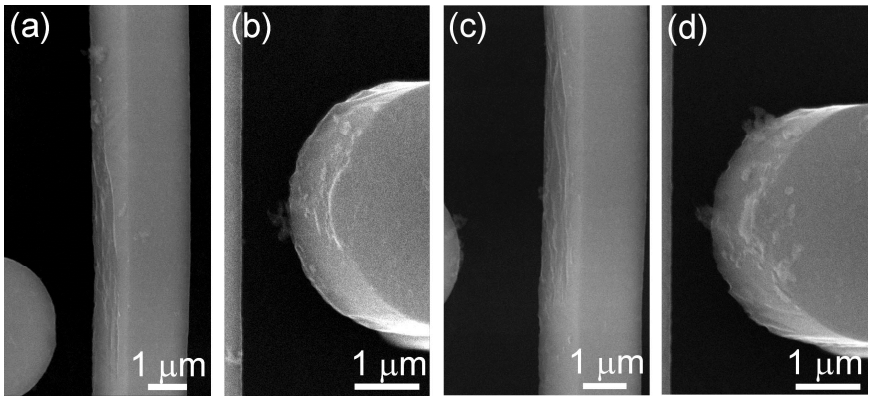

Figure 5: SEM micrographs of: (a) Mode I device at 750,000 cycles showing the beam (a) and the post (b); Mode II device at 150,000 cycles (2 failures) showing the beam (c) and the post (d). All images are shown at 30 degree tilt.

The shape and depth of the grooves of the worn areas of the sidewall devices were studied in the AFM; data were used to calculate the nano-scale wear volume. These volumes were converted into dimensionless wear coefficients to mitigate differences in operating conditions using Archard's law [11,12]. Wear coefficient data calculated from different devices as a function of wear cycles (Fig. 6) show that after an initial rise to ~10^{-4} at approximately 100,000 cycles, the coefficients decay to a value of 10^{-5} as the accumulated wear cycles increase.

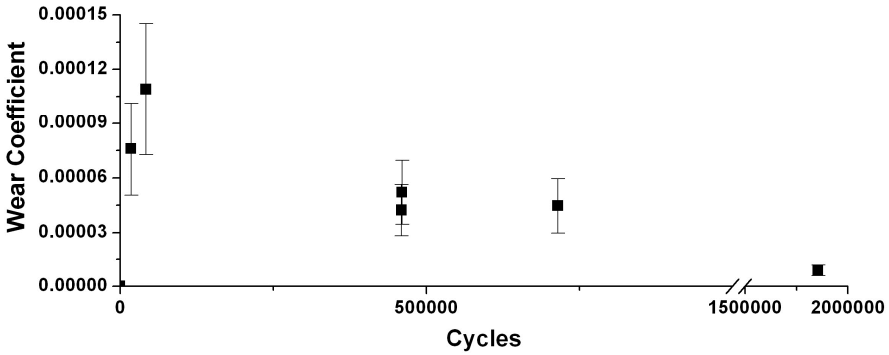

Figure 6: Variation in the wear coefficient for polysilicon showing an initial rapid increase followed by a steady decrease with increasing number of wear cycles (normal contact forces P ~ 3-6 μN). After Ref. [9].

DISCUSSION

The evolution of the dynamic coefficient of friction for Mode I (Fig. 2) devices shows strong resemblance to the classical tribological theory for a harder (more wear resistant) slider worn against a softer (less wear resistant) specimen [13]. In the classical case, abrasion between surface asperities leads to an initial increase in friction coefficient whereas a steady-state regime is reached when equilibrium between wear particle generation and the fracture of surface asperities and existing wear particles is reached. In this micro/nano-scale case, an initial adhesive wear regime, in which the monolayer coating and oxide is worn away, is know to exist which changes into abrasive wear at <10,000 cycles [9] before the steady-state coefficient of friction has reached its peak. After this peak, which corresponds to the peak in highest wear coefficient as well as surface roughness [9], there is a decreasing chance of new wear particles being formed because of interactions of previously formed wear particles between the contact surfaces. This results in a steady-state friction regime for Mode I devices. This peak followed by a lower steady–state regime here arises from a difference in the wear resistance between the post and the beam. Despite the fact that both the beam and post consist of polysilicon, the effective wear resistance of the post is higher than that of the beam as shown by the fact that wear of the post is always found to be far smaller than wear of the beam (no grooves on the posts in Figure and Ref. [9]). This is because the contact width on the post is ~100-500 nm which corresponds to about one grain (grain size ~ 450 nm [14]), while the contact length of the beam is ~ 5-7 μm which corresponds to 10-15 grains. This makes the sampling region of the post single crystal silicon, whereas for the beam it is polycrystalline, which has weakening stress-concentrating grain-boundary cusps.

For Mode II devices (3 out of 7 devices tested), the initial development of the dynamic coefficient of friction is the same as for Mode I devices (4 out of 7 tested devices tested); however at the Mode I peak value, friction coefficients for Mode II devices increase more followed by device failure (Fig. 3). Whether a device will run in Mode I or Mode II is expected to be governed by local variations in the surface morphology of the sidewall contacts and particularly the effect of wear particles, which could lower the real area of contact when trapped between the surfaces. In Mode I the real area of contact at the highest friction point is likely lowered by these particles, allowing for continued operation.

The decay of the static coefficient of friction after stopping worn devices (Fig. 4) is attributed to re-growth of the native oxide layer, which was removed during wear. The growth of a native SiO_2 layer in air on single crystal silicon is in the order of 6 Å after 30 mins [15], which is the time before a drop in static friction is observed (Fig. 4). After 10^3-10^4 mins, it reaches about double that thickness [15], at which point the static friction coefficient reaches its lower limit. This shows that when this lower friction coefficient limit is reached further growth of the SiO_2 layer has no more influence on the static coefficient of friction. The data in Fig. 4 also illustrate the effect of oxidation during the wear process, a mechanism that has been used to describe wear in ambient air [*e.g.*, 16]. Because the coefficient of friction only starts decreasing significantly after 30 mins it is unlikely that the oxide growth has any significant influence on friction or wear during cycling in ambient air.

CONCLUSIONS

On-chip n^+-type polysilicon micron-scale sidewall specimens have been used to study the dynamic coefficient of friction under μN loads in ambient air. It is concluded that first the

coating and silicon oxide wears away, after which the coefficient of friction increases to a peak value of 0.3 ± 0.1 at ~10^5 cycles. Some devices are able to cycle for millions of cycles (Mode I) after reaching a steady-state coefficient of friction of 0.25 ± 0.10, while other devices stop functioning significantly earlier due to increasing friction force (Mode II). Whether a device runs in Mode I or II is governed by local variation in the contact morphology due to microstructure variations. Additionally, it was found that re-oxidation of polysilicon only has a significant influence on the coefficient of friction some 30 mins after the device has stopped, indicating that oxide re-growth does not influence wear during cycling.

ACKNOWLEDGEMENTS

This work was funded by the Director, Office of Science, Office of Basic Energy Sciences, Division of Materials Sciences and Engineering, of the U.S. Department of Energy under Contract No. DE-AC02-05CH11231 at the Lawrence Berkeley National Laboratory (LBNL) at the National Center for Electron Microscopy and the Molecular Foundry (special thanks to Drs. Ashby and Ogletree), both operated at LBNL with the support of the U.S. Department of Energy under Contract No. DE-AC02-05CH11231. Support for MTD from Sandia National Laboratories is also gratefully acknowledged. Sandia is a multi-program laboratory operated by Sandia Corporation, a Lockheed-Martin Company, for the U.S. Department of Energy's National Nuclear Security Administration under contract DE-AC04-94AL85000.

REFERENCES

1. B. Bhushan, H.W. Liu, *Nanotechnology.* **15**, 1785 (2004).
2. N. Mulaf, K. Williams, "An Introduction to Microelectromechanical Systems Engineering," Artech House Publishers, 2004.
3. A.D. Jr. Romig, M.T. Dugger, P.J. McWhorter, *Acta. Mater.* **51**, 5837 (2003).
4. S.H. Kim, D.B. Asay, M.T. Dugger, *Nano Today*. **2**, 22 (2007).
5. D.H. Alsem, O.N. Pierron, E.A. Stach, C.L. Muhlstein, R.O. Ritchie, *Adv. Eng. Mater.* **9,** 15 (2007).
6. D.C. Senft, and M.T. Dugger, *Proc. of SPIE Micromachined Devices and Components III* **3224**, 31 (1997).
7. U. Srinivasan, M.R. Houston, R.T. Howe, R.Maboudian, *J. Microelectromech. Syst.***7**,252 (1998).
8. W.R. Ashurst, C. Yau, C. Carraro, R. Maboudian, M.T. Dugger, *J. Microelectromech. Syst.* **9**, 41 (2001).
9. D. H. Alsem, M. T. Dugger, E. A. Stach, R. O. Ritchie, *J. Microelectomech. Syst.* Submitted (2007).
10. S.J. Timpe, K. Komvopoulos, *Rev. Sci. Instrum.* **78**, 065106 (2007).
11. J.F. Archard, *J. Appl. Phys.* **24**, 981 (1953).
12. J.F. Archard, *J. Appl. Phys.* **32,** 1420 (1961).
13. N.P. Suh, H.C. Sin, *Wear*. **69**, 91 (1981).
14. D.H. Alsem, B.L. Boyce, E.A. Stach, R.O. Ritchie, *Sens. Actuators A*. Submitted (2008).
15. W.B. Ying, Y. Mizokawa, Y. Kamiura, K. Kawamoto, W.Y. Yang, *Appl. Surf. Sci.* **181**, 1 (2001).
16. S.T. Patton, J.S. Zabinski, *Tribology International*. **15**, 373 (2002).